Title: CryoEM Structure with ATP Synthase Enables Late-stage Diversification of Cruentaren A

Authors: Xiaozheng Dou; Hui Guo; Terin D'Amico; Leah Abdullah; Chitra Subramanian; Bhargav A. Patel; Mark Cohen; John L. Rubinstein; Brian Blagg

To be cited as: 10.1002/chem.202300262

Link to VoR: https://doi.org/10.1002/chem.202300262

CryoEM Structure with ATP Synthase Enables Late-stage Diversification of Cruentaren A

Xiaozheng Dou[a]§, Hui Guo[b]§, Terin D'Amico[a], Leah Abdallah[c], Chitra Subramanian[d], Bhargav A. Patel[a], Mark Cohen[d], John L. Rubinstein[b,e], and Brian S. J. Blagg*[a]

[a] Dr. X. Dou, T. D'Amico, Dr. B. Patel, Prof. B. S. J. Blagg

Department of Chemistry and Biochemistry, The University of Notre Dame, Notre Dame, Indiana, 46556, United States

Corresponding author's email: bblagg@nd.edu

[b] Dr. H. Guo, Prof. J. L. Rubinstein

Molecular Medicine Program, The Hospital for Sick Children, Toronto, Canada;

Department of Medical Biophysics, University of Toronto, Ontario, Canada;

[c] L. Abdullah

Department of Surgery, University of Michigan, Ann Arbor, MI, 48109 United States;

[d] Dr. C. Subramanian, Prof. Mark Cohen

Departments of Surgery and Bioengineering, Carle Illinois College of Medicine, University of Illinois, Urbana-Champaign, 61801, United States:

[e] Prof. J. L. Rubinstein

Departments of Biochemistry, University of Toronto, Ontario, Canada

§X.D. and H.G. contributed equally to this manuscript. All authors have given approval to the final version of the manuscript.

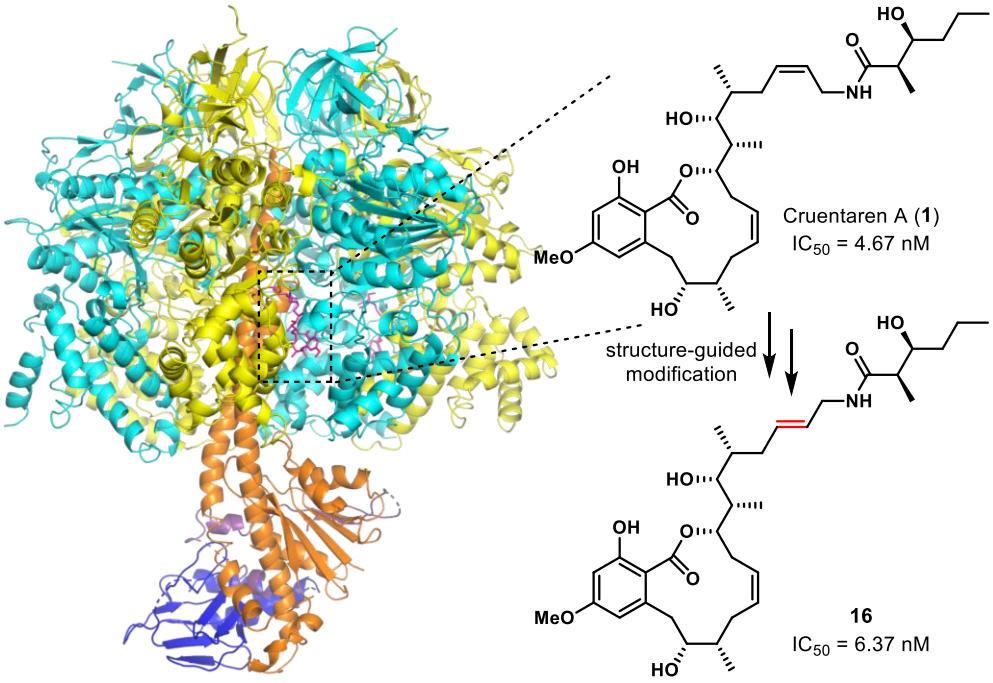

Abstract

Cruentaren A is a natural product that exhibits potent antiproliferative activity against various cancer cell lines, yet its binding site within ATP synthase remained unknown, limiting the development of improved analogues as anticancer agents. Herein, we report the cryogenic electron microscopy (cryoEM) structure of cruentaren A bound to ATP synthase, which allowed for the design of new inhibitors via semisynthetic modification. Examples of cruentaren A derivatives include a *trans*-alkene isomer, which was found to exhibit similar activity as cruentaren A against three cancer cell lines as well as several other analogues that retained potent inhibitory activity. Together, these studies provide a foundation for the generation of cruentaren A derivatives as potential therapeutics for the treatment of cancer.

Introduction

Cruentaren A (**1**, Figure 1) is a macrolide natural product that was isolated from the myxobacterium *Byssovorax cruenta* by Höfle et al and disrupts the cellular process of oxidative phosphorylation (OXPHOS) via selective inhibition of mitochondrial adenosine triphosphate

synthase (ATP synthase, F_1F_O-ATPase).[1] The natural product is a promising anticancer agent that exhibits subnanomolar antiproliferative activity against multiple cancer cell lines, while manifesting IC_{50} values greater than 500 nM against the normal cell lines, HEK293 and MRC5.[2] Cruentaren A contains a resorcinol-derived, 12-membered macrocyclic lactone and a *cis*-allyl amide side chain. It has also been reported that cruentaren A undergoes rapid and quantitative translactonization onto the C9 hydroxyl to form the biologically inactive isomer, cruentaren B.[1] Additional structure-activity relationship (SAR) studies on cruentaren A could provide insights into the development of new ATP synthase inhibitors for the treatment of cancer.[3]

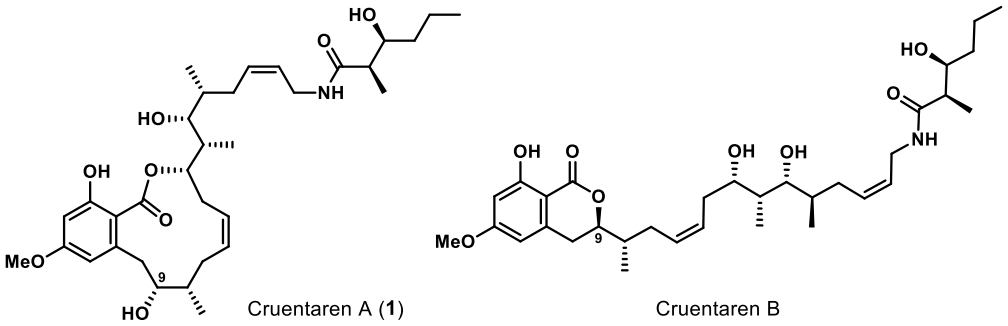

Figure 1. Structures of cruentaren A and cruentaren B.

ATP synthase is a multiprotein complex that contains 29 subunits.[4] The subunits are divided into two functional domains; a membrane-bound F_O domain which translocates protons through the mitochondrial membrane, and a soluble catalytic F_1 domain that harnesses energy from a proton electrochemical gradient to synthesize ATP. The F_O domain is subdivided into three groups; the rotor ring, the peripheral stalk, and the supernumerary subunit. The F_1 domain can be subdivided into the F_1 catalytic head and the F_1 central stalk. The F_1 catalytic head is a six-fold pseudo-symmetric ring that includes three alternating α and β subunits, while the central stalk is composed of γ, δ, and ε subunits.

The major function of ATP synthase is to generate ATP for cellular energy of which more than 95% of cellular ATP is produced under aerobic conditions (OXPHOS). Moreover, the

synthase facilitates the activity of other proteins, such as heat shock protein 90 (Hsp90).[5] It was reported that ATP synthase is a partner protein for Hsp90 and plays an important role during the maturation of Hsp90-dependent client proteins.[5d] Furthermore, ATP synthase collaborates with the Hsp90 homodimer to assemble a heteroprotein complex that is necessary for folding select protein substrates.[6]

It was demonstrated that cruentaren A disrupts interactions between ATP synthase and Hsp90 and consequently induces Hsp90-dependent client protein degradation, which provides a new opportunity to modulate the Hsp90 protein folding machinery.[2] Unfortunately, the mechanism by which cruentaren A binds and inhibits ATP synthase remained unknown, and has hampered the development of improved analogues. We recently reported the synthesis and evaluation of 12 cruentaren A analogues in an effort to establish preliminary SAR for simplification of the molecule (Figure 2).[7] However, all 12 compounds were significantly less active, resulting in minimal insight into this promising anticancer agent. Therefore, the structure of cruentaren A bound to ATP synthase is needed to rationally improve upon cruentaren A's promising anticancer activity.

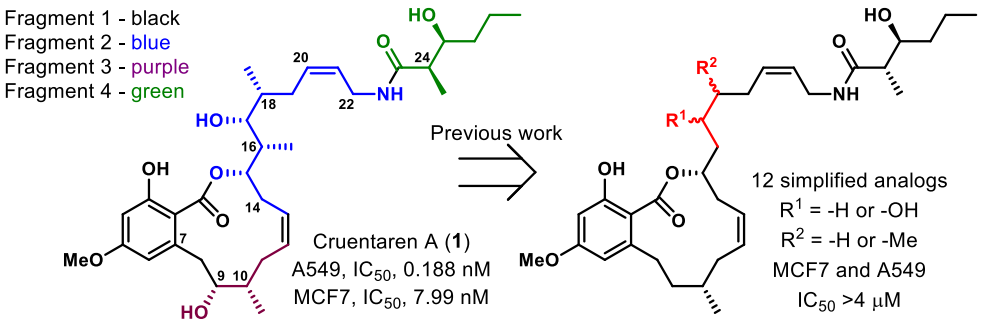

Figure 2. Previous SAR studies on cruentaren A. Cruentaren A is colored into 4 fragments based on our previously reported total synthesis. Our previously reported simplifications along fragment 2 are colored in red.

Results and Discussion

Identification of Binding Sites via Cryogenic Electron Microscopy (cryoEM). It was confirmed that cruentaren A inhibits detergent solubilized *Saccharomyces cerevisiae* ATP synthase with an IC_{50} of ~75 nM via ATPase assays (supplementary Figure 1). Although previous reports have indicated that cruentaren A binds the F_1 region of ATP synthase[1b], the exact binding site was unknown. Therefore, we determined a cryoEM structure of yeast ATP synthase (~20 mg/mL) in the presence of 100 μM of cruentaren A at 2.9 Å resolution (supplementary Figure 2 and 3, supplementary Table 1). At this concentration, the molar ratio of protein to drug is ~1:3, and densities corresponding to cruentaren A are found at both the $\alpha_{TP}\beta_{TP}$ and $\alpha_{DP}\beta_{DP}$ interfaces of the F_1 region (Figure 3a). This observation is not surprising given the structural similarity of the two interfaces.[8] To investigate whether one binding site exhibits higher cruentaren A binding affinity, a 4.5 Å resolution structure of yeast ATP synthase (~10 mg/mL) was determined with 25 μM of cruentaren A (supplementary Figure 2 and 3, supplementary Table 1). At this concentration, the protein to drug molar ratio is approximately 2:3. The resulting structure shows strong drug density at the $\alpha_{TP}\beta_{TP}$ interface and weak density at the $\alpha_{DP}\beta_{DP}$ interface, suggesting that the $\alpha_{TP}\beta_{TP}$ interface has higher binding affinity to cruentaren A.

Since the $\alpha_{TP}\beta_{TP}$ interface was determined to be the high-affinity binding site, the following discussion is focused on interactions of cruentaren A at the $\alpha_{TP}\beta_{TP}$ interface. Although cruentaren A binds at the $\alpha_{TP}\beta_{TP}$ interface next to the nucleotide binding site of the β subunit, it does not appear to affect the binding of ADP (Figure 3b). In the β_{TP} subunit, the distance between the sugar backbone of ADP and the *cis*-allyl amide of cruentaren A is only 4.3 Å. Furthermore, the macrocyclic ring is directed towards the C terminus of the β subunit and faces towards the solvent-exposed region. Fragment 2 occupies the space between helix 1 of the C terminus in the α_{TP} subunit and helix 4 of the C terminus in the β_{TP} subunit[8], wherein the distance between the C16 methyl

group and α_{TP} is 3.7 Å and the distance between the C18 methyl group and β_{TP} is 3.9 Å, which may explain why fragment deletions are detrimental to cruentaren A's biological activity due to potential loss of hydrophobic interactions.[7]

Although previous SAR studies with cruentaren A have identified some inhibitors via diverted total syntheses, the interactions between cruentaren A and amino acids within the ATP synthase remained unknown.[7, 9] During the course of our studies, it was determined that the methyl group at C16 interacts with α_{TP}-Val369, α_{TP}-Leu394, and α_{TP}-Ala397, while the C18 methyl group interacts with the methylene of β_{TP}-Phe424. Additionally, the hydroxyl group at C17 forms a hydrogen bond with α_{TP}-Lys393 (Figure 3c). Fragment 4 is buried deep inside the binding pocket and interacts with hydrophobic residues of the α_{TP} subunit, including α_{TP}-Ile345, α_{TP}-Val336, and α_{TP}-Phe353 (Figure 3c), which explains prior SAR studies that demonstrated steric bulk on fragment 4 is not tolerated.[9b] Additional hydrogen-bond interactions were also found between the C25 hydroxyl group and both β_{TP}-Arg337 and β_{TP}-Glu341, while the amide interacts with α_{TP}-Gln351. Together, these observations show that the high affinity binding conformation of cruentaren A to ATP synthase is mediated primarily through hydrophobic interactions with α_{TP} (Figure 3d). By binding to and stabilizing the nucleotide-bound $\alpha_{TP}\beta_{TP}$ interface, cruentaren A inhibits ATP synthase in an uncompetitive manner, without direct interactions with the rotor.

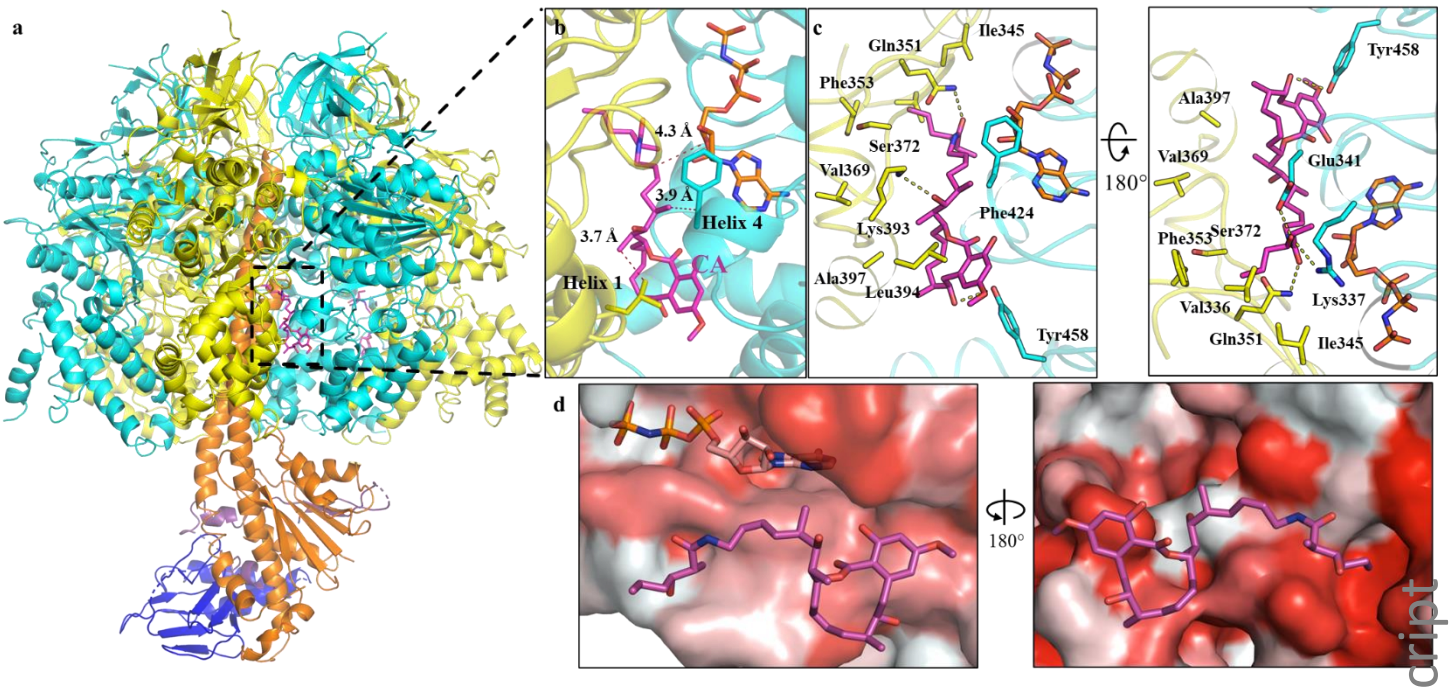

Figure 3. Structure of cruentaren A-bound yeast ATP synthase. (a) Atomic model of the F_1 region of ATP synthase bound to cruentaren A. Cruentaren A is shown in magenta. (b) Close-up view of the cruentaren A binding site. The red dotted lines are the distance. CA is cruentaren A. (c) The binding-site residues. The yellow dot lines are the hydrogen-bond interactions. (d) Electrostatic potentials mapped onto the binding sites. Left is cruentaren A with the β_{TP} subunit. Right is cruentaren A with the α_{TP} subunit. Hydrophobic residues are in red. Hydrophilic residues are in white.

The cryoEM structure not only validated prior SAR studies, but also provided additional insights into the binding site that could help optimize the activity of cruentaren A. For instance, the cryoEM structure suggests that oxidation or esterification of the C9 alcohol of cruentaren A could be accommodated within the binding pocket and enable hydrogen-bond interactions with amino acids α_{TP}-Glu401, β_{TP}-Tyr458, and β_{TP}-His455 (Figure 4a). In addition, it was determined that the side-chain alkene (C20-C21) faces an unexplored and amphiphilic pocket containing Val373 of the α_{TP} subunit and Tyr345 and Phe424 from the β_{TP} subunit (Figure 4b).

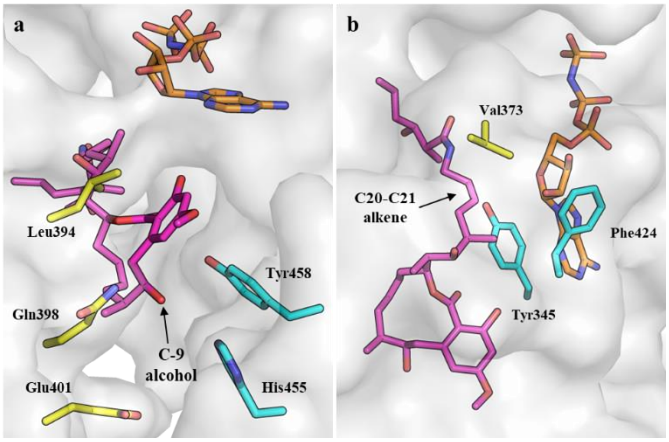

Figure 4. Cruentaren A in ATP synthase. (a) Post at the C9 alcohol and (b) post at the side-chain alkene (C20-C21). Amino acids from the α_{TP} subunit are yellow and from the β_{TP} subunit are blue.

Late-stage Modification of Cruentaren A Derivatives. The alcohols and alkenes present in cruentaren A were modified by semisynthetic approaches to further elucidate SAR using the cryoEM structure as a guide for optimization. Since cruentaren A undergoes rapid rearrangement with the C9 alcohol, the alcohol was converted to the corresponding ester or ketone to mask reactivity. Gratifyingly, oxidation readily occurred at C9, allowing selective modification at this location. Consequently, cruentaren A was oxidized with one equivalent of Dess-Martin periodinane to convert the C9 alcohol into the corresponding ketone, which resulted in **2** (Scheme 1).[10]

Conditions were probed to couple amino acids with the alcohols present in cruentaren A as an alternative method to increase interactions with ATP synthase, especially along the macrocycle as it faces a solvent-exposed channel. When cruentaren A was treated with two equivalents of Fmoc-protected glycine acyl chloride[11], esterification occurred at both the phenol and C9 alcohol. Conveniently, treatment of these intermediates with piperidine in dichloromethane not only removed the Fmoc protecting groups[12], but also cleaved the more labile phenolic ester and provided **3**. Amino acids containing hydrophobic side chains such as alanine, valine, and phenylalanine were attached to C9 in an effort to probe for steric interactions via compounds **4**-**6**.

Dual esterification of C9 and C25 readily occurred with three equivalents of Fmoc-protected phenylalanine chloride, which upon cleavage of the phenolic ester produced derivative **7**.

Cruentaren A was treated with 3 equivalents of acetic anhydride (Ac_2O) to install acetyl groups onto the phenol as well as onto the C9 and C25 alcohols. Chemoselective deacetylation of the phenolic ester with 1,1,3,3-tetramethylguanidine (TMG) in acetonitrile provided compound **8**.[13] Moreover, with 5 equivalents of Ac_2O, a fully esterified analogue (**9**) of cruentaren A was achieved after solvolysis. Interestingly, when **8** or **9** were dissolved in methanol, cleavage of the C25 ester was observed and led to **10** and **11**, respectively.

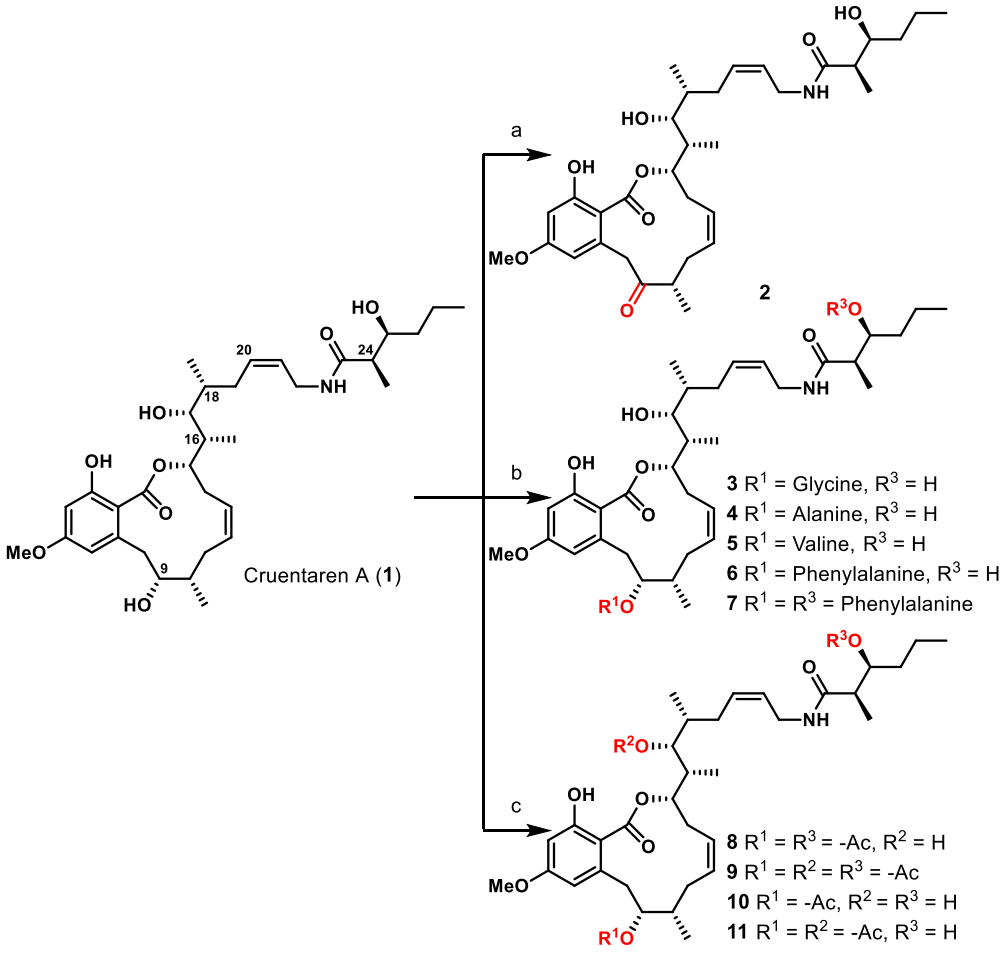

Scheme 1. a) Dess-Martin periodinane, pyridine, DCM, 0 °C to rt, 30%; b) i. Fmoc-protected amino acid chloride, DIPEA, DMAP, DCM, 41-85%; ii. piperidine, DCM, 60-90%; c) i. 3 or 5 eq. Ac_2O, DIPEA, DMAP, DCM, 51-70%; ii. TMG, MeCN, 50 °C, 30-60%; iii. MeOH, 30%. DIPEA = *N*,*N*-diisopropylethylamine, DMAP = 4-dimethylaminopyridine.

Additional modifications were performed to understand the biological activity conferred by the C20-C21 *cis*-alkene, as it faces an amphiphilic pocket. Cruentaren A was fully hydrogenated with 10% palladium on carbon (Pd/C) in ethyl acetate to provide **12** (Scheme 2). In contrast, dihydroxylation of cruentaren A led to a rearrangement that produced an analogue of cruentaren B, which is the inactive microcyclic isomer of cruentaren A.[14] Therefore, cruentaren A was treated with methoxyacetyl chloride to protect the phenol and alcohols, which prevented rearrangement and allowed for subsequent modification of the side-chain alkene.[15] Dihydroxylation of **13** with catalytic osmium tetroxide and *N*-methylmorpholine *N*-oxide (NMO) afforded the corresponding diol.[16] After solvolysis under basic conditions, compound **14** was obtained. Alternatively, protected cruentaren A (**13**) was treated with diethylzinc and diiodomethane to direct cyclopropanation at C20-C21, which upon solvolysis provided **15**.[17] Finally, isomerization of compound **13** with a palladium catalyst led to formation of the *trans*-alkene at C20-C21, which underwent solvolysis to furnish **16**.[18]

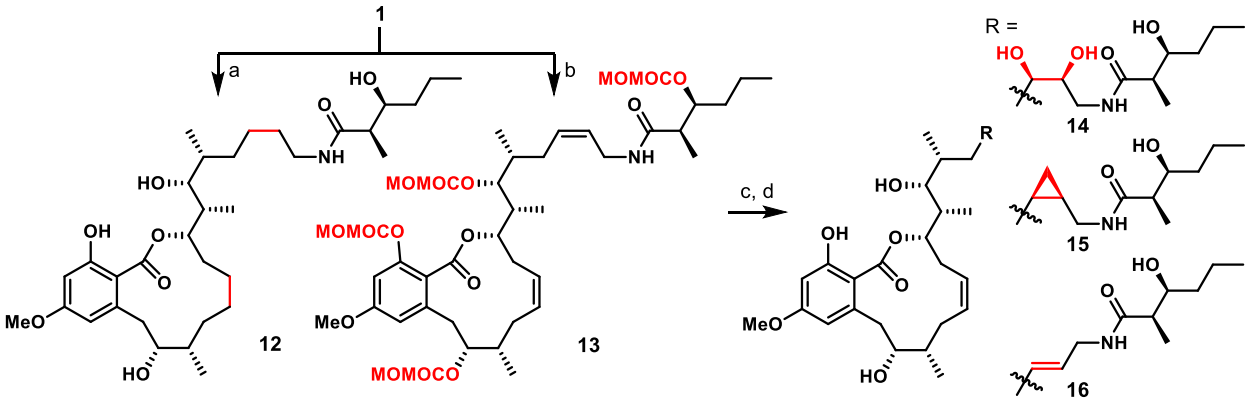

Scheme 2. a) Pd/C, H_2, EtOAc, 86%; b) MOMCOCl, DIPEA, DMAP, DCM, 63%; c) i. OsO_4, NMO, Acetone/t-BuOH/water, 90%; ii. Et_2Zn, diiodomethane, 0 °C; iii. $Pd(MeCN)_2Cl_2$, DCM, 82%. d) K_2CO_3, MeOH, 35-81%.

Upon preparation of the library of cruentaren A analogues, their antiproliferative activities were determined against various cancer cell lines. The cancer cell lines MCF7 (breast cancer), K562 (leukemia), and A549 (lung cancer) were selected due to their dependency on F_1F_O ATP

synthase for energy production.[19] Cruentaren A (**1**) was included as a control and the IC_{50} values obtained from these studies are listed in Table 1. The IC_{50} values manifested by cruentaren A were 4.67 nM, 1.50 nM, and 0.75 nM as determined against MCF7, K562 and A549 cell lines, respectively, similar to previously reported values.[2]

Several of the synthetic analogues demonstrated comparable activity as the natural product. Oxidation of the C9 alcohol to ketone **2**, resulted in reduced potency against all three cell lines. However, the IC_{50} value for glycine analogue **3** was 14.8 nM against the K562 cell line, which is 10-fold lower than cruentaren A and suggests that the primary amine may mediate hydrogen-bond interactions with F_1F_O ATP synthase. Derivative **3** manifested a higher IC_{50} value (87.5 nM) against MCF7 cells as compared to K562 cells. However, the introduction of amino acids did not significantly affect antiproliferative activity against MCF7 cells as **4-6** exhibited IC_{50} values between 50 and 100 nM, but manifested a loss in potency against the K562 cell line when compared to **3** (50~100 fold). Surprisingly, the bis esterified analogue (**7**) manifested improved activity when compared to **6** with IC_{50} values of 51 nM against MCF7 and 65 nM against K562 cells.

Esterification of cruentaren A decreases antiproliferative activity as demonstrated via **8-11**. Esterification at C9 (**10**) lead to decreased antiproliferative activity and IC_{50} values of 0.17 μM, 1.16 μM, and 1.96 μM against the MCF7, K562 and A549 cell lines, respectively. In contrast, esterification of the C25 hydroxyl group (**8**) maintained activity against all three cancer cell lines when compared to **10**. Finally, esterification of the C16 hydroxyl led to inactive compounds at 4 μM as demonstrated by **9** and **11**, which indicates limited potential to modify the C16 position.

Analogues **12-15** were synthesized to explore the amphiphilic region in ATP synthase. The fully saturated analogue **12** manifested less antiproliferative activity than cruentaren A. Although

it was initially hypothesized that hydroxyl groups could provide an additional source of hydrogen-bond interactions with ATP synthase, compound **14** exhibited a ~40-fold reduction in activity. Cyclopropanated analogue **15** manifested a 100-fold decrease in activity as compared to cruentaren A, which is likely the result of an undesired conformation. Surprisingly, a similar level of activity was retained with the *trans*-alkene **16,** especially against MCF7 cells wherein it manifested an IC_{50} value of 6.37 nM. The antiproliferative activity of cruentaren A is most potent against A549 and least potent against MCF7, however, most of these analogues demonstrated the opposite trend, wherein all but **3** were most active against MCF7 cells and least active against the A549 cell line.

Table 1. IC_{50} values of cruentaren A analogues.

	IC_{50} values (nM)		
	MCF7	**K562**	**A549**
1	4.67	1.50	0.750
2	972	1283	1637
3	87.5	14.8	1740
4	55.5	1321	2447
5	101	968	1334
6	114	1120	1285
7	51.3	64.6	2458
8	574	1283	3360
9	>4000	>4000	>4000
10	174	1158	1958
11	>4000	>4000	>4000
12	179	1390	4000
14	189	1267	1540
15	520	1121	1240
16	6.37	48.3	1750

Previous studies have demonstrated that cruentaren A induced the degradation of Hsp90-dependent client proteins in MCF7 cells upon 48-hour incubation.[2] Therefore, **4**, **16**, and geldanamycin were evaluated by the same procedure, and all of these compounds induced a dose-dependent degradation of the Hsp90-dependent client proteins phosphorylated Akt (pAkt), Cyclin D1 and GLUT1, as shown in Figure 5. However, the levels of Hsp70 and Hsp90 were increased upon treatment with geldanamycin and indicates induction of the heat shock response. Treatment

with **4** and **16** led to the degradation of the client proteins at concentrations similar to the antiproliferative IC_{50} values linking cell viability to Hsp90 inhibition. After 48 hours of treatment with the cruentaren A analogues, Hsp70, Hsp90 and ATP synthase remained at the same level as vehicle control (0.25% DMSO). These studies are consistent with our previous report that disruption of Hsp90-ATP synthase interactions induced Hsp90-dependent client protein degradation without induction of Hsp70 or Hsp90 levels, indicating that these analogues maintain the same mechanism of action as cruentaren A.

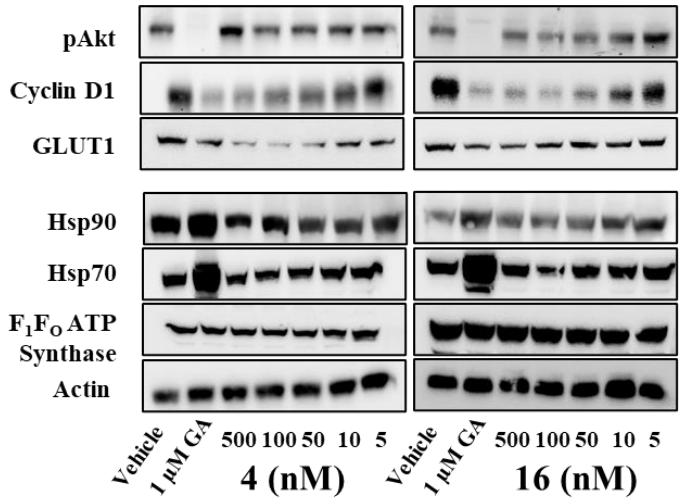

Figure 5. Western Blot analysis for Hsp90 client proteins (pAkt, Cyclin D1 and GLUT1) and Hsp70, Hsp90, and F_1F_O ATP synthase using MCF7 cell lysates after 48 h of incubation with the indicated amount of **4** and **16**, vehicle (0.25% DMSO), or 1 μM geldanamycin (GA).

Conclusion

While many natural products have been shown to manifest potent anticancer activity *in vitro*, there are numerous factors that can hinder their translation to the clinic. For instance, the natural product Hsp90 inhibitor, geldanamycin, was transformed into 17-N-allylamino-17-demethoxygeldanamycin (17-AAG), which underwent clinical investigation.[20] However, all *pan*-Hsp90 inhibitors activate the pro-survival heat-shock response and result in increased levels of Hsp90.[21] In contrast to direct inhibition of the N-terminal ATP binding site, disruption of Hsp90-

ATP synthase protein-protein interactions represents as an alternative approach to inhibit Hsp90 without concomitant induction of the heat shock response.[5d] In addition, recent studies support the OXPHOS pathway, including ATP synthase, as a promising target for the development of new cancer therapeutics.[22] Therefore, cruentaren A manifests a dual mechanism of action for treating cancer, which supports its potential as an anticancer agent. In this manuscript, the binding site of cruentaren A has been elucidated and can now enable a rational, structure-based approach for the optimization of cruentaren A analogues.

Although natural products often possess exciting activity and unique pharmacokinetic properties, they often require significant modification to become a viable drug candidate for the clinic.[23] In this work, cruentaren A was modified based on the co-structure with ATP synthase to produce a small library of semisynthetic derivatives (**2-12** and **14-16**), which were investigated for their antiproliferative activity against various cancer cell lines. Analogue **16** was shown to manifest similar activity (IC_{50} = 6.37 nM) against the MCF7 cell line as cruentaren A and highlights the utility of this approach. When combined with the structural insights and present SAR studies on cruentaren A, this work provides a promising foundation to develop new analogues via the co-structure of cruentaren A bound to ATP synthase.

Experimental Section

Safety statement and general experimental details. No unexpected or unusually high safety hazards were encountered. All reactions were carried out in oven-dried glassware under an argon atmosphere unless otherwise stated. Commercially available anhydrous solvent and reagents were utilized without any further purification. THF, DCM, MeCN, and toluene were purified *via* a MBRAUN solvent purification system. Flash column chromatography was performed using silica gel (40-63 µM particle size). ^{1}H and ^{13}C NMR spectra were recorded at 400 and 101 MHz, respectively, on a Bruker Avance III HD 400 Nanobay or a Bruker Avance III HD 500 using $CDCl_3$ purchased from Cambridge Isotope Laboratories, Inc., with the solvent as an internal standard ($CDCl_3$ at 7.27 ppm for ^{1}H and 77.16 ppm for ^{13}C). Data are reported as p = pentet, q = quartet, t = triplet, d = doublet, s = singlet, brs = broad singlet, m = multiplet; coupling constant(s) in Hz. High-resolution mass spectral data were obtained on a time-of-flight mass spectrometer,

and analysis was performed using electrospray ionization. Optical rotations were recorded with a Perkin Elmer polarimeter at 589 nm at 25 °C with concentration reported as g/100 mL.

Compound data for final products

(2R,3S)-3-hydroxy-N-((5R,6R,7S,Z)-6-hydroxy-7-((3S,8S,Z)-14-hydroxy-12-methoxy-8-methyl-1,9-dioxo-3,4,7,8,9,10-hexahydro-1H-benzo[c][1]oxacyclododecin-3-yl)-5-methyloct-2-en-1-yl)-2-methylhexanamide (**2**): Pyridine (3.0 equiv) and Dess–Martin periodinane (1.0 equiv) were added to a solution of cruentaren A (1.0 equiv) in DCM at 0 °C. The solution was stirred for 15 min at 0 °C and then was allowed to warm up to ambient temperature for overnight. The reaction was quenched with aq. sat. $Na_2S_2O_3$ and aq. $NaHCO_3$. The aqueous layer was extracted by DCM (5 mL × 4) and the combined organic layer was dried over Na_2SO_4, filtered, and concentrated down. The residue was purified by HPLC to give the product **2**. ^{1}H NMR (800 MHz, Chloroform-*d*) δ 11.88 (s, 1H), 6.42 (d, *J* = 2.6 Hz, 1H), 6.23 (d, *J* = 2.6 Hz, 1H), 6.16 (t, *J* = 5.8 Hz, 1H), 5.67 – 5.57 (m, 1H), 5.53 (ddd, *J* = 11.5, 10.3, 6.6 Hz, 1H), 5.46 – 5.39 (m, 1H), 5.37 (ddd, *J* = 12.0, 11.5, 4.6 Hz, 1H), 5.31 (ddd, *J* = 11.5, 7.0, 2.7 Hz, 1H), 4.12 (d, *J* = 17.7 Hz, 1H), 3.96 (dddd, *J* = 14.9, 7.4, 5.7, 1.3 Hz, 1H), 3.85 (ddd, *J* = 15.4, 8.0, 4.8 Hz, 2H), 3.82 (s, 3H), 3.64 (d, *J* = 17.6 Hz, 1H), 3.45 (ddd, *J* = 9.2, 6.5, 2.0 Hz, 1H), 3.25 (d, *J* = 3.3 Hz, 1H), 2.91 (d, *J* = 6.7 Hz, 1H), 2.82 (td, *J* = 13.7, 10.3, 7.0 Hz, 1H), 2.69 (ddd, *J* = 13.7, 11.5, 7.5 Hz, 1H), 2.57 (ddq, *J* = 7.1, 2.2 Hz, 1H), 2.32 (ddd, *J* = 15.1, 9.2, 7.0 Hz, 1H), 2.28 – 2.20 (m, 3H), 2.14 (qdd, *J* = 7.6, 6.9, 2.0 Hz, 1H), 1.77 – 1.68 (m, 2H), 1.52 – 1.42 (m, 2H), 1.35 – 1.25 (m, 2H), 1.14 (d, *J* = 7.1 Hz, 3H), 1.08 (d, *J* = 7.0 Hz, 3H), 0.93 (d, *J* = 7.0 Hz, 3H), 0.93 (t, *J* = 7.1 Hz, 3H), 0.87 (d, *J* = 6.9 Hz, 3H). ^{13}C NMR (201 MHz, Chloroform-*d*) δ 212.5, 176.6, 171.0, 166.1, 164.2, 138.7, 131.0, 130.8, 127.6, 126.9, 113.1, 105.9, 100.1, 79.1, 73.9, 71.9, 55.6, 50.7, 44.9, 44.6, 38.1, 36.7, 36.6, 35.9, 31.0, 30.8, 30.1, 19.4, 19.3, 16.0, 14.2, 11.3, 9.1. HRMS (ESI/Q-TOF) m/z: $[M + Na]^+$ Calcd for $C_{33}H_{49}NNaO_8$ 610.3350; Found 610.3350. $[\alpha]^{20}_D$ = –22.1 (*c* = 0.15, DCM).

Synthesis of ***3-7***. Piperidine (20.0 equiv) in DCM (20%v/v) was dropwise added to the desired cruentaren A analogues (1.0 equiv) in a 5 mL vial at 0 °C. The reaction was allowed to warm up to room temperature for 2 hr. The reaction was purified by flash chromatography (5% MeOH in DCM) to give the corresponding product **3-7**.

(3S,8S,9R,Z)-14-hydroxy-3-((2S,3R,4R,Z)-3-hydroxy-8-((2R,3S)-3-hydroxy-2-methylhexanamido)-4-methyloct-6-en-2-yl)-12-methoxy-8-methyl-1-oxo-3,4,7,8,9,10-hexahydro-1H-benzo[c][1]oxacyclododecin-9-yl glycinate (**3**): ^{1}H NMR (800 MHz, Chloroform-*d*) δ 11.62 (s, 1H), 6.32 (dd, *J* = 2.7, 0.9 Hz, 1H), 6.23 (d, *J* = 2.7 Hz, 1H), 6.17 – 6.02 (m, 1H), 5.63 – 5.54 (m, 2H), 5.54 – 5.49 (m, 1H), 5.42 (dt, *J* = 12.0, 7.1 Hz, 1H), 5.33 – 5.16 (m, 1H), 4.98 (dt, *J* = 11.4, 2.6 Hz, 1H), 3.91 (dt, *J* = 13.7, 6.5 Hz, 1H), 3.87 – 3.84 (m, 2H), 3.83 – 3.79 (m, 2H), 3.78 (s, 3H), 3.49 – 3.40 (m, 1H), 3.26 (d, *J* = 17.9 Hz, 1H), 3.22 – 3.16 (m, 1H), 3.13 (d, *J* = 17.9 Hz, 1H), 2.85 (dt, *J* = 25.5, 11.9 Hz, 1H), 2.44 (dd, *J* = 13.3, 11.5 Hz, 1H), 2.39 – 2.32 (m, 1H), 2.32 – 2.25 (m, 3H), 2.24 – 2.17 (m, 1H), 2.07 – 2.02 (m, 2H), 1.99 (d, *J* = 14.7 Hz, 1H), 1.71 – 1.67 (m, 1H), 1.52 – 1.44 (m, 2H), 1.36 – 1.29 (m, 2H), 1.15 (d, *J* = 7.1 Hz, 3H), 1.03 (d, *J* = 6.8 Hz, 3H), 0.93 (t, *J* = 7.2 Hz, 3H), 0.92 (d, *J* = 7.0 Hz, 3H), 0.81 – 0.78 (m, 3H). ^{13}C NMR (126 MHz, Chloroform-*d*) δ 176.64, 171.57, 165.83, 163.34, 142.63, 131.39, 131.24, 126.86, 126.62, 113.28, 99.65, 78.13, 77.12, 74.91, 72.05, 55.59, 45.06, 43.97, 39.28, 37.12, 36.74, 36.65, 35.97,

33.73, 31.87, 31.15, 29.96, 19.44, 16.33, 14.82, 14.25, 11.40, 8.84. HRMS (ESI/Q-TOF) m/z: [M + H]$^+$ Calcd for $C_{35}H_{55}N_2O_9$ 647.3902, found 647.3893. $[\alpha]^{20}_D$ = +2.31 (*c* = 0.13, DCM).

(3S,8S,9R,Z)-14-hydroxy-3-((2S,3R,4R,Z)-3-hydroxy-8-((2R,3S)-3-hydroxy-2-methylhexanamido)-4-methyloct-6-en-2-yl)-12-methoxy-8-methyl-1-oxo-3,4,7,8,9,10-hexahydro-1H-benzo[c][1]oxacyclododecin-9-yl D-alaninate (**4**): ^{1}H NMR (800 MHz, Chloroform-*d*) δ 11.62 (s, 1H), 6.31 (d, *J* = 2.7 Hz, 1H), 6.26 (d, *J* = 2.7 Hz, 1H), 6.10 (t, *J* = 5.8 Hz, 1H), 5.62 – 5.58 (m, 1H), 5.56 (ddt, *J* = 10.1, 6.5, 1.7 Hz, 1H), 5.52 (ddt, *J* = 11.2, 7.1, 2.4 Hz, 1H), 5.44 – 5.39 (m, 1H), 5.32 – 5.28 (m, 1H), 4.95 (ddd, *J* = 11.6, 3.1, 2.0 Hz, 1H), 3.90 (dddd, *J* = 14.7, 7.3, 5.6, 1.4 Hz, 1H), 3.87 – 3.82 (m, 2H), 3.80 (dd, *J* = 13.4, 1.9 Hz, 1H), 3.77 (s, 3H), 3.47 (dd, *J* = 9.1, 2.2 Hz, 1H), 3.34 (q, *J* = 6.8 Hz, 1H), 3.12 (s, 1H), 2.84 (dt, *J* = 14.5, 11.6 Hz, 1H), 2.49 (dd, *J* = 13.4, 11.6 Hz, 1H), 2.39 – 2.32 (m, 1H), 2.28 (qd, *J* = 7.1, 5.7, 3.5 Hz, 3H), 2.22 – 2.15 (m, 1H), 2.08 – 2.02 (m, 2H), 1.98 (d, *J* = 14.5 Hz, 1H), 1.87 (s, 1H), 1.69 (ddt, *J* = 9.2, 6.9, 3.5 Hz, 1H), 1.50 – 1.43 (m, 2H), 1.35 – 1.30 (m, 2H), 1.15 (d, *J* = 7.1 Hz, 3H), 1.03 (d, *J* = 4.4 Hz, 3H), 1.02 (d, *J* = 4.5 Hz, 3H), 0.93 (t, *J* = 7.2 Hz, 3H), 0.91 (d, *J* = 7.1 Hz, 3H), 0.79 (d, *J* = 6.8 Hz, 3H). ^{13}C NMR (201 MHz, Chloroform-*d*) δ 176.6, 176.0, 171.5, 165.8, 163.3, 142.5, 131.4, 131.2, 126.8, 126.6, 113.9, 104.9, 99.4, 78.1, 76.8, 74.9, 72.0, 55.5, 50.3, 45.0, 39.2, 37.1, 36.7, 36.5, 35.9, 33.8, 31.8, 30.9, 29.9, 20.5, 19.4, 16.3, 14.7, 14.2, 11.3, 8.8. HRMS (ESI/Q-TOF) m/z: [M + H]$^+$ Calcd for $C_{36}H_{57}N_2O_9$ 661.4059, found 661.4050. $[\alpha]^{20}_D$ = +1.02 (*c* = 0.59, DCM).

(3S,8S,9R,Z)-14-hydroxy-3-((2S,3R,4R,Z)-3-hydroxy-8-((2R,3S)-3-hydroxy-2-methylhexanamido)-4-methyloct-6-en-2-yl)-12-methoxy-8-methyl-1-oxo-3,4,7,8,9,10-hexahydro-1H-benzo[c][1]oxacyclododecin-9-yl D-valinate (**5**): ^{1}H NMR (800 MHz, Chloroform-*d*) δ 11.62 (s, 1H), 6.33 (d, *J* = 2.7 Hz, 1H), 6.31 (d, *J* = 2.7 Hz, 1H), 6.15 (t, *J* = 5.8 Hz, 1H), 5.65 (tt, *J* = 11.7, 2.8 Hz, 1H), 5.59 (td, *J* = 10.5, 9.2, 1.3 Hz, 1H), 5.54 (ddd, *J* = 10.9, 4.8, 2.1 Hz, 1H), 5.44 (dt, *J* = 10.8, 7.1 Hz, 1H), 5.32 (ddd, *J* = 11.7, 5.4, 2.0 Hz, 1H), 4.94 (dt, *J* = 11.8, 2.3 Hz, 1H), 3.96 – 3.90 (m, 1H), 3.90 – 3.83 (m, 2H), 3.83 – 3.77 (m, 1H), 3.80 (s, 3H), 3.48 (dd, *J* = 9.1, 2.2 Hz, 1H), 3.16 (d, *J* = 4.4 Hz, 1H), 2.86 (dt, *J* = 14.1, 11.6 Hz, 1H), 2.53 (dd, *J* = 13.4, 11.7 Hz, 1H), 2.43 – 2.34 (m, 1H), 2.34 – 2.26 (m, 3H), 2.23 (dd, *J* = 8.0, 1.7 Hz, 1H), 2.14 (d, *J* = 8.2 Hz, 1H), 2.07 – 1.95 (m, 2H), 1.83 – 1.75 (m, 1H), 1.71 (dtd, *J* = 8.9, 6.7, 4.0 Hz, 1H), 1.56 – 1.42 (m, 2H), 1.39 – 1.31 (m, 2H), 1.17 (d, *J* = 7.2 Hz, 3H), 1.04 (d, *J* = 6.9 Hz, 3H), 0.95 (t, *J* = 7.0 Hz, 3H), 0.92 (d, *J* = 7.0 Hz, 3H), 0.84 (d, *J* = 6.9 Hz, 3H), 0.80 (d, *J* = 6.8 Hz, 3H), 0.44 (d, *J* = 6.8 Hz, 3H). ^{13}C NMR (201 MHz, Chloroform-*d*) δ 176.5, 171.3, 165.6, 163.2, 142.4, 131.3, 131.0, 126.7, 126.3, 113.7, 104.6, 99.3, 78.0, 74.7, 71.8, 59.9, 55.3, 44.8, 39.1, 36.9, 36.5, 36.2, 35.8, 33.6, 31.7, 31.3, 30.7, 29.7, 19.6, 19.2, 16.1, 15.7, 14.6, 14.7, 11.2, 8.6. HRMS (ESI/Q-TOF) m/z: [M + H]$^+$ Calcd for $C_{38}H_{61}N_2O_9$ 689.4366, found 689.4372. $[\alpha]^{20}_D$ = –3.38 (*c* = 0.47, DCM).

(3S,8S,9R,Z)-14-hydroxy-3-((2S,3R,4R,Z)-3-hydroxy-8-((2R,3S)-3-hydroxy-2-methylhexanamido)-4-methyloct-6-en-2-yl)-12-methoxy-8-methyl-1-oxo-3,4,7,8,9,10-hexahydro-1H-benzo[c][1]oxacyclododecin-9-yl D-phenylalaninate (**6**): ^{1}H NMR (800 MHz, Chloroform-*d*) δ 11.66 (s, 1H), 7.25 – 7.20 (m, 2H), 7.21 – 7.16 (m, 1H), 6.87 (dd, *J* = 8.1, 1.3 Hz, 2H), 6.37 (d, *J* = 2.7 Hz, 1H), 6.25 (d, *J* = 2.7 Hz, 1H), 6.11 (t, *J* = 6.0 Hz, 1H), 5.64 – 5.60 (m, 1H), 5.57 (dddt, *J* = 10.6, 8.5, 7.0, 1.7 Hz, 1H), 5.53 (dtd, *J* = 11.4, 5.8, 5.2, 2.2 Hz, 1H), 5.45 – 5.38 (m, 1H), 5.31 (ddd, *J* = 11.7, 5.5, 1.9 Hz, 1H), 4.94 (ddd, *J* = 11.7, 3.0, 1.9 Hz, 1H), 3.91 (dddd, *J* = 14.7, 7.3, 5.6, 1.4 Hz, 1H), 3.88 – 3.80 (m, 3H), 3.60 (s, 3H), 3.56 – 3.51 (m, 1H), 3.48 (dd, *J* = 9.2, 2.1 Hz, 1H), 2.91 – 2.80 (m, 1H), 2.72 (dd, *J* = 13.7, 4.5 Hz, 1H), 2.55 (dd, *J* = 13.5,

11.7 Hz, 1H), 2.47 (dd, *J* = 13.7, 7.8 Hz, 1H), 2.37 (q, *J* = 12.4 Hz, 1H), 2.29 (qd, *J* = 7.1, 2.8 Hz, 3H), 2.24 – 2.18 (m, 1H), 2.14 (q, *J* = 4.1 Hz, 1H), 2.07 – 2.01 (m, 1H), 1.99 (d, *J* = 14.5 Hz, 1H), 1.70 (dtd, *J* = 9.1, 6.8, 4.1 Hz, 1H), 1.51 – 1.43 (m, 1H), 1.37 – 1.29 (m, 2H), 1.15 (d, *J* = 7.1 Hz, 4H), 1.02 (d, *J* = 6.9 Hz, 4H), 0.93 (t, *J* = 7.1 Hz, 3H), 0.92 (d, *J* = 7.1 Hz, 3H), 0.79 (d, *J* = 6.8 Hz, 3H). ^{13}C NMR (126 MHz, Chloroform-*d*) δ 176.6, 174.5, 171.5, 165.9, 163.4, 142.5, 137.1, 131.4, 131.2, 129.3, 128.5, 126.8, 126.5, 114.2, 104.8, 99.5, 78.2, 74.9, 72.0, 55.6, 55.4, 45.0, 40.6, 39.2, 37.1, 36.7, 36.2, 35.9, 33.7, 31.8, 30.9, 29.8, 19.4, 16.3, 14.7, 14.2, 11.3, 8.8. HRMS (ESI/Q-TOF) m/z: $[M + H]^+$ Calcd for $C_{42}H_{61}N_2O_9$ 737.4371, found 737.4372. $[\alpha]^{20}_D$ = +2.90 (*c* = 0.25, DCM).

(2R,3S)-1-(((5R,6R,7S,Z)-7-((3S,8S,9R,Z)-9-((D-phenylalanyl)oxy)-14-hydroxy-12-methoxy-8-methyl-1-oxo-3,4,7,8,9,10-hexahydro-1H-benzo[c][1]oxacyclododecin-3-yl)-6-hydroxy-5-methyloct-2-en-1-yl)amino)-2-methyl-1-oxohexan-3-yl D-phenylalaninate (**7**): ^{1}H NMR (800 MHz, Chloroform-*d*) δ 7.33 – 7.30 (m, 2H), 7.28 – 7.23 (m, 1H), 7.24 – 7.20 (m, 5H), 7.21 – 7.16 (m, 1H), 6.90 – 6.81 (m, 2H), 6.36 (d, *J* = 2.7 Hz, 1H), 6.24 (d, *J* = 2.7 Hz, 1H), 5.84 (t, *J* = 5.8 Hz, 1H), 5.64 – 5.59 (m, 1H), 5.58 – 5.46 (m, 2H), 5.39 – 5.24 (m, 2H), 5.03 (dt, *J* = 8.1, 4.9 Hz, 1H), 4.98 – 4.89 (m, 1H), 3.86 – 3.78 (m, 2H), 3.78 – 3.73 (m, 1H), 3.72 (dd, *J* = 7.9, 6.2 Hz, 1H), 3.59 (s, 3H), 3.54 (dd, *J* = 7.7, 4.4 Hz, 1H), 3.44 (dd, *J* = 9.2, 2.3 Hz, 1H), 3.11 (dd, *J* = 13.6, 6.3 Hz, 1H), 2.85 (dd, *J* = 13.6, 8.0 Hz, 1H), 2.84 – 2.78 (m, 1H), 2.72 (dd, *J* = 13.7, 4.4 Hz, 1H), 2.54 (dd, *J* = 13.4, 11.6 Hz, 1H), 2.47 (dd, *J* = 13.7, 7.8 Hz, 1H), 2.37 (dd, *J* = 26.7, 13.9 Hz, 1H), 2.32 (dd, *J* = 7.1, 4.9 Hz, 2H), 2.29 – 2.24 (m, 1H), 2.23 – 2.17 (m, 1H), 2.16 – 2.11 (m, 1H), 2.03 – 1.95 (m, 2H), 1.89 (p, *J* = 6.2 Hz, 0H), 1.69 (dtd, *J* = 9.3, 6.7, 4.2 Hz, 1H), 1.52 (dddd, *J* = 11.2, 8.9, 5.0, 2.9 Hz, 2H), 1.31 – 1.26 (m, 1H), 1.24 – 1.18 (m, 1H), 1.09 (d, *J* = 7.0 Hz, 3H), 1.01 (d, *J* = 6.9 Hz, 3H), 0.89 (d, *J* = 7.0 Hz, 3H), 0.88 (t, *J* = 7.4 Hz, 3H), 0.78 (d, *J* = 6.8 Hz, 3H). ^{13}C NMR (201 MHz, Chloroform-*d*) δ 174.4, 174.2, 172.9, 171.4, 165.9, 163.3, 142.5, 137.4, 137.0, 131.2, 131.0, 129.5, 129.3, 128.9, 128.5, 127.1, 126.8, 126.7, 114.1, 104.9, 99.5, 78.2, 77.4, 76.1, 74.4, 56.7, 55.6, 55.4, 44.7, 41.5, 40.6, 39.4, 36.9, 36.8, 36.1, 33.6, 32.9, 31.8, 30.9, 29.7, 19.2, 16.4, 14.7, 14.0, 13.2, 9.0. HRMS (ESI/Q-TOF) m/z: $[M + H]^+$ Calcd for $C_{51}H_{70}N_3O_{10}$ 884.5056, found 884.5055. $[\alpha]^{20}_D$ = –4.84 (*c* = 0.52, DCM).

*Synthesis of **8-11***. A solution of TMG (4.0 equiv) in anhydrous MeCN was added to phenyl acetate (1.0 equiv) in a 5 mL vial. The solution was stirred for 2 h at 50 °C. The solvent was evaporated under reduced pressure and the crude was purified by HPLC to give the desired **8** or **9**. Crude **8** or **9** was dissolved into MeOH and stirred at room temperature for 12 h. The crude was purified by HPLC to give the products **10** or **11**.

(2R,3S)-1-(((5R,6R,7S,Z)-7-((3S,8S,9R,Z)-9-acetoxy-14-hydroxy-12-methoxy-8-methyl-1-oxo-3,4,7,8,9,10-hexahydro-1H-benzo[c][1]oxacyclododecin-3-yl)-6-hydroxy-5-methyloct-2-en-1-yl)amino)-2-methyl-1-oxohexan-3-yl acetate (**8**): ^{1}H NMR (800 MHz, Chloroform-*d*) δ 11.6 (s, 1H), 6.3 (d, 1H), 6.3 (d, *J* = 2.2 Hz, 1H), 5.9 (s, 1H), 5.6 (q, *J* = 15.1, 13.1 Hz, 2H), 5.5 (t, *J* = 10.9 Hz, 1H), 5.4 (q, *J* = 8.0 Hz, 1H), 5.3 – 5.3 (m, 1H), 5.1 (td, *J* = 7.3, 5.4, 3.2 Hz, 1H), 4.9 (d, *J* = 11.1 Hz, 1H), 3.9 (dt, *J* = 13.5, 6.7 Hz, 1H), 3.8 (dt, *J* = 13.5, 6.7 Hz, 1H), 3.8 (d, *J* = 13.0 Hz, 1H), 3.8 (s, 3H), 3.6 – 3.4 (m, 1H), 2.8 (q, *J* = 11.3, 9.4 Hz, 2H), 2.5 – 2.4 (m, 2H), 2.4 (t, *J* = 12.8 Hz, 1H), 2.3 – 2.2 (m, 2H), 2.2 (dt, *J* = 15.0, 7.9 Hz, 1H), 2.1 (s, 3H), 2.0 (d, *J* = 6.6 Hz, 2H), 2.0 (d, *J* = 14.6 Hz, 1H), 1.8 (s, 3H), 1.7 (t, *J* = 7.5 Hz, 1H), 1.5 – 1.5 (m, 2H), 1.3 (q, *J* = 8.8, 8.1 Hz, 2H), 1.1 (d, *J* = 7.0 Hz, 3H), 1.0 (d, *J* = 6.9 Hz, 3H), 0.9 (d, *J* = 7.1 Hz, 3H), 0.9 (t, *J* = 7.4 Hz, 3H), 0.8

(d, *J* = 6.8 Hz, 3H). ^{13}C NMR (201 MHz, Chloroform-*d*) δ 173.5, 171.7, 170.9, 170.1, 165.8, 163.4, 142.9, 131.5, 131.3, 126.8, 126.6, 113.2, 105.2, 99.7, 78.1, 75.2, 74.9, 55.6, 45.3, 39.4, 37.1, 37.0, 36.6, 34.0, 33.7, 31.9, 31.0, 30.0, 23.0, 21.4, 21.2, 19.2, 16.1, 14.6, 13.8, 13.2, 9.0. HRMS (ESI/Q-TOF) m/z: $[M + H]^+$ Calcd for $C_{37}H_{56}NO_{10}$ 674.3899; Found 674.3906. $[\alpha]^{20}_D$ = +2.19 (c = 0.42, DCM).

(2R,3R,4R,Z)-2-((3S,8S,9R,Z)-9-acetoxy-14-hydroxy-12-methoxy-8-methyl-1-oxo-3,4,7,8,9,10-hexahydro-1H-benzo[c][1]oxacyclododecin-3-yl)-8-((2R,3S)-3-acetoxy-2-methylhexanamido)-4-methyloct-6-en-3-yl acetate (**9**): ^{1}H NMR (500 MHz, Chloroform-*d*) δ 11.67 (s, 1H), 6.33 (d, *J* = 2.7 Hz, 1H), 6.27 (d, *J* = 2.7 Hz, 1H), 5.65 (t, *J* = 5.5 Hz, 1H), 5.58 (td, *J* = 10.8, 2.3 Hz, 1H), 5.45 (ddd, *J* = 10.8, 3.5, 1.1 Hz, 1H), 5.43 – 5.31 (m, 2H), 5.10 – 5.03 (m, 2H), 4.97 (dd, *J* = 7.6, 2.6 Hz, 1H), 4.90 (dt, *J* = 11.3, 2.6 Hz, 1H), 3.79 (s, 3H), 3.84 – 3.69 (m, 3H), 2.70 – 2.59 (m, 1H), 2.50 – 2.39 (m, 2H), 2.34 – 2.20 (m, 3H), 2.09 (s, 3H), 2.06 (s, 3H), 2.04 – 1.99 (m, 2H), 1.98 – 1.92 (m, 1H), 1.91 – 1.83 (m, 2H), 1.81 (s, 3H), 1.55 – 1.50 (m, 2H), 1.40 – 1.19 (m, 2H), 1.14 (d, *J* = 7.0 Hz, 3H), 1.04 (d, *J* = 6.8 Hz, 3H), 0.98 (d, *J* = 7.1 Hz, 3H), 0.89 (t, *J* = 7.3 Hz, 3H), 0.79 (d, *J* = 6.6 Hz, 3H). ^{13}C NMR (126 MHz, Chloroform-*d*) δ 173.1, 171.4, 170.8, 170.1, 166.0, 163.5, 143.1, 132.0, 131.2, 126.9, 126.0, 113.4, 104.8, 99.7, 77.4, 76.0, 75.8, 75.3, 56.6, 55.6, 45.3, 37.9, 36.7, 36.6, 36.0, 34.0, 33.8, 31.8, 30.6, 28.4, 21.5, 21.3, 21.2, 19.1, 16.4, 14.9, 14.1, 13.7, 10.7. HRMS (ESI/Q-TOF) m/z: $[M + H]^+$ Calcd for $C_{39}H_{58}NO_{11}$ 716.4004; Found 716.4022. $[\alpha]^{20}_D$ = –6.67 (c = 0.15, DCM).

(3S,8S,9R,Z)-14-hydroxy-3-((2S,3R,4R,Z)-3-hydroxy-8-((2R,3S)-3-hydroxy-2-methylhexanamido)-4-methyloct-6-en-2-yl)-12-methoxy-8-methyl-1-oxo-3,4,7,8,9,10-hexahydro-1H-benzo[c][1]oxacyclododecin-9-yl acetate (**10**): ^{1}H NMR (800 MHz, Chloroform-*d*) δ 11.62 (s, 1H), 6.33 (d, *J* = 2.4 Hz, 1H), 6.26 (s, 1H), 6.11 (s, 1H), 5.70 – 5.54 (m, 2H), 5.50 (s, 1H), 5.42 (d, *J* = 9.7 Hz, 1H), 5.29 (d, *J* = 11.8 Hz, 1H), 4.90 (d, *J* = 11.3 Hz, 1H), 3.90 (dd, *J* = 14.7, 7.3 Hz, 1H), 3.84 (d, *J* = 19.7 Hz, 2H), 3.78 (d, *J* = 1.3 Hz, 4H), 3.47 (s, 1H), 3.14 (s, 1H), 2.84 (q, *J* = 12.1 Hz, 1H), 2.66 (s, 1H), 2.42 (t, *J* = 12.3 Hz, 1H), 2.35 (q, *J* = 12.8 Hz, 1H), 2.27 (d, *J* = 13.2 Hz, 3H), 2.23 – 2.14 (m, 1H), 2.03 (s, 2H), 1.97 (d, *J* = 14.9 Hz, 1H), 1.82 (d, *J* = 1.2 Hz, 3H), 1.70 (s, 1H), 1.50 – 1.44 (m, 2H), 1.33 (d, *J* = 11.3 Hz, 2H), 1.15 (dd, *J* = 7.2, 1.3 Hz, 3H), 1.03 (d, *J* = 6.9 Hz, 3H), 0.95 – 0.92 (m, 3H), 0.93 – 0.90 (m, 3H), 0.90 – 0.69 (m, 3H). ^{13}C NMR (201 MHz, Chloroform-*d*) δ 176.4, 171.4, 169.8, 165.5, 163.1, 142.6, 131.3, 131.1, 126.6, 126.1, 113.0, 104.9, 99.4, 77.8, 76.0, 74.8, 71.8, 55.3, 44.8, 39.1, 36.9, 36.5, 36.3, 35.7, 33.4, 31.7, 30.7, 29.8, 20.9, 19.2, 16.1, 14.6, 14.0, 11.2, 8.6. HRMS (ESI/Q-TOF) m/z: $[M + H]^+$ Calcd for $C_{39}H_{58}NO_{11}$ 632.3799; Found 632.3810. $[\alpha]^{20}_D$ = +2.35 (c = 0.17, DCM).

(2R,3R,4R,Z)-2-((3S,8S,9R,Z)-9-acetoxy-14-hydroxy-12-methoxy-8-methyl-1-oxo-3,4,7,8,9,10-hexahydro-1H-benzo[c][1]oxacyclododecin-3-yl)-8-((2R,3S)-3-hydroxy-2-methylhexanamido)-4-methyloct-6-en-3-yl acetate (**11**): ^{1}H NMR (800 MHz, Chloroform-*d*) δ 11.67 (s, 1H), 6.32 (d, *J* = 2.7 Hz, 1H), 6.27 (d, *J* = 2.7 Hz, 1H), 5.87 (t, *J* = 4.6 Hz, 1H), 5.62 – 5.52 (m, 1H), 5.46 – 5.42 (m, 1H), 5.42 – 5.39 (m, 1H), 5.39 – 5.33 (m, 1H), 5.06 (dd, *J* = 11.6, 5.6 Hz, 1H), 4.97 (dd, *J* = 7.6, 2.5 Hz, 1H), 4.92 – 4.86 (m, 1H), 3.86 (d, *J* = 8.0 Hz, 1H), 3.79 (s, 3H), 3.80 – 3.76 (m, 2H), 3.73 (dt, *J* = 14.2, 6.2 Hz, 1H), 3.43 (d, *J* = 3.2 Hz, 1H), 2.64 (q, *J* = 12.0 Hz, 1H), 2.45 (t, *J* = 12.4 Hz, 1H), 2.28 (d, *J* = 2.7 Hz, 3H), 2.23 (d, *J* = 14.5 Hz, 1H), 2.09 (s, 3H), 2.01 (d, *J* = 14.5 Hz, 2H), 1.95 (d, *J* = 14.2 Hz, 1H), 1.91 – 1.82 (m, 2H), 1.81 (s, 3H), 1.52 – 1.44 (m, 2H), 1.40 – 1.28 (m, 2H), 1.16 (d, *J* = 7.2 Hz, 3H), 1.04 (d, *J* = 6.9 Hz, 3H), 0.98 (d, *J* = 7.0 Hz, 3H), 0.93 (t, *J* =

7.0 Hz, 3H), 0.80 (d, *J* = 6.5 Hz, 3H).^{13}C NMR (201 MHz, Chloroform-*d*) δ 176.6, 171.4, 171.3, 170.0, 165.9, 163.4, 143.0, 131.9, 131.3, 126.6, 125.9, 113.3, 104.7, 99.6, 76.9, 75.9, 75.7, 71.8, 55.5, 44.7, 37.7, 36.6, 36.3, 35.9, 35.9, 33.7, 31.7, 30.6, 28.3, 21.5, 21.1, 19.4, 16.3, 14.8, 14.2, 11.2, 10.6.HRMS (ESI/Q-TOF) m/z: $[M + H]^+$ Calcd for $C_{37}H_{56}NO_{10}$ 674.3899; Found 674.3906. $[\alpha]_D^{20} = -2.27$ (c = 0.22, DCM).

Synthesis of ***12***. 10% Pd/C (0.1 equiv) was added to a solution of cruentaren A (1.0 equiv) in EtOAc. The reaction was stirred under a hydrogen balloon for 2 h. The solution was filtered through a pad of celite and washed with EtOAc. The filtrate was concentrated under reduced pressure and was purified by HPCL to give the product **12**.

(2R,3S)-N-((5R,6R,7S)-7-((3S,8S,9R)-9,14-dihydroxy-12-methoxy-8-methyl-1-oxo-3,4,5,6,7,8,9,10-octahydro-1H-benzo[c][1]oxacyclododecin-3-yl)-6-hydroxy-5-methyloctyl)-3-hydroxy-2-methylhexanamide (**12**): ^{1}H NMR (800 MHz, Chloroform-*d*) δ 11.48 (s, 1H), 6.38 (d, *J* = 2.6 Hz, 1H), 6.35 (d, *J* = 2.7 Hz, 1H), 5.73 (s, 1H), 5.12 (dd, *J* = 9.9, 4.4 Hz, 1H), 3.92 – 3.87 (m, 1H), 3.85 (d, *J* = 8.3 Hz, 1H), 3.81 (s, 3H), 3.78 (d, *J* = 9.7 Hz, 1H), 3.45 – 3.39 (m, 1H), 3.37 (s, 1H), 3.15 (dp, *J* = 20.2, 6.4 Hz, 2H), 2.27 – 2.21 (m, 2H), 2.13 (d, *J* = 7.4 Hz, 1H), 2.02 (td, *J* = 16.4, 8.0 Hz, 1H), 1.84 (s, 0H), 1.48 (t, *J* = 6.9 Hz, 3H), 1.44 (s, 3H), 1.33 (dt, *J* = 24.0, 9.6 Hz, 8H), 1.15 (dd, *J* = 7.5, 1.5 Hz, 3H), 1.07 (s, 2H), 0.96 (d, *J* = 6.8 Hz, 3H), 0.93 (dt, *J* = 7.3, 3.6 Hz, 7H), 0.75 (d, *J* = 6.7 Hz, 3H). ^{13}C NMR (201 MHz, Chloroform-*d*) δ 176.5, 171.8, 165.6, 163.5, 144.2, 111.8, 105.4, 99.7, 82.2, 75.0, 71.7, 55.4, 44.7, 38.9, 38.4, 37.2, 36.8, 35.8, 31.5, 30.0, 29.7, 26.6, 25.5, 23.8, 23.4, 19.2, 15.9, 15.0, 14.0, 11.1, 9.9. HRMS (ESI/Q-TOF) m/z: $[M + H]^+$ Calcd for $C_{33}H_{56}NO_8$ 594.4000; Found 594.4001. $[\alpha]^{20}_D$ = +11.0 (c = 0.30, DCM).

Synthesis of **14-16**. K_2CO_3 (10 equiv) was added to a stirred solution of the crude compound (1.0 equiv) in MeOH at 0 °C. The resulting solution was stirred at the same temperature for 2 hrs, then at room temperature for 5 hrs. The reaction mixture was then diluted with DCM (2 mL) and was quenched by saturated aqueous ammonium chloride (2 mL). The layers were separated, and the aqueous layer extracted with DCM (3 × 2 mL). The combined organic layers were dried over Na_2SO_4, filtered, and concentrated down. The residue purified by HPLC or flash chromatography (5% MeOH in DCM) to give the product **14-16**, sometimes only one of the diastereomers could be obtained in pure form.

(2R,3S)-N-((2S,3R,5R,6R,7S)-7-((3S,8S,9R,Z)-9,14-dihydroxy-12-methoxy-8-methyl-1-oxo-3,4,7,8,9,10-hexahydro-1H-benzo[c][1]oxacyclododecin-3-yl)-2,3,6-trihydroxy-5-methyloctyl)-3-hydroxy-2-methylhexanamide (**14**): ^{1}H NMR (800 MHz, Chloroform-*d*) δ 11.54 (s, 1H), 6.54 (s, 1H), 6.37 (d, *J* = 2.6 Hz, 1H), 6.31 (d, *J* = 2.7 Hz, 1H), 5.50 (t, *J* = 10.7 Hz, 1H), 5.44 (ddt, *J* = 13.6, 8.9, 2.9 Hz, 1H), 5.26 (q, *J* = 4.9, 4.5 Hz, 1H), 3.89 – 3.84 (m, 1H), 3.81 (s, 3H), 3.75 (dd, *J* = 12.7, 1.8 Hz, 1H), 3.65 (dt, *J* = 10.8, 2.3 Hz, 1H), 3.61 (d, *J* = 10.3 Hz, 1H), 3.49 (s, 1H), 3.46 (s, 2H), 3.43 (dd, *J* = 8.9, 2.0 Hz, 1H), 3.32 (d, *J* = 14.4 Hz, 1H), 2.92 – 2.79 (m, 1H), 2.41 (s, 1H), 2.38 – 2.30 (m, 1H), 2.28 – 2.21 (m, 2H), 2.03 (p, *J* = 5.8 Hz, 2H), 1.96 (d, *J* = 14.7 Hz, 1H), 1.76 (q, *J* = 7.0, 6.2 Hz, 1H), 1.66 – 1.57 (m, 2H), 1.54 – 1.43 (m, 4H), 1.41 – 1.35 (m, 2H), 1.41 – 1.27 (m, 2H), 1.16 (d, *J* = 7.2 Hz, 3H), 1.03 (d, *J* = 6.8 Hz, 3H), 0.93 (t, *J* = 7.2 Hz, 3H), 0.89 (d, *J* = 6.9 Hz, 3H), 0.83 (d, *J* = 6.8 Hz, 3H). ^{13}C NMR (201 MHz, Chloroform-*d*) δ 178.3, 171.6, 165.8, 163.6, 143.8, 132.2, 125.7, 112.4, 104.8, 99.7, 78.1, 76.4, 74.5, 73.0, 72.0, 71.0, 55.4, 45.1, 41.9, 39.5, 38.3, 37.8, 36.7, 35.7, 35.0, 31.6, 29.9, 19.3, 18.1, 14.2, 14.0, 11.1, 8.4. HRMS (ESI/Q-TOF)

m/z: $[M + Na]^+$ Calcd for $C_{33}H_{53}NNaO_{10}$ 646.3562; Found 646.3560. $[\alpha]^{20}_D$ = +6.43 (*c* = 0.23, DCM).

(2R,3S)-N-(((1R,2R)-2-((2R,3R,4S)-4-((3S,8S,9R,Z)-9,14-dihydroxy-12-methoxy-8-methyl-1-oxo-3,4,7,8,9,10-hexahydro-1H-benzo[c][1]oxacyclododecin-3-yl)-3-hydroxy-2-methylpentyl)cyclopropyl)methyl)-3-hydroxy-2-methylhexanamide (**15**): ^{1}H NMR (800 MHz, Chloroform-*d*) δ 11.56 (s, 1H), 6.40 (d, *J* = 2.7 Hz, 1H), 6.34 (d, *J* = 2.7 Hz, 1H), 6.02 (s, 1H), 5.54 (t, *J* = 11.3 Hz, 1H), 5.46 (ddt, *J* = 13.7, 9.0, 2.6 Hz, 1H), 5.28 (ddd, *J* = 11.7, 5.2, 1.9 Hz, 1H), 3.90 (dt, *J* = 8.8, 3.2 Hz, 1H), 3.83 (s, 3H), 3.76 (d, *J* = 12.7 Hz, 1H), 3.69 – 3.64 (m, 1H), 3.54 (ddd, *J* = 8.5, 6.2, 2.4 Hz, 1H), 3.44 (d, *J* = 3.2 Hz, 1H), 3.36 (ddd, *J* = 13.3, 7.1, 5.7 Hz, 1H), 3.11 (dddd, *J* = 24.7, 13.6, 7.7, 4.9 Hz, 1H), 2.90 (q, *J* = 12.1 Hz, 1H), 2.36 (q, *J* = 12.7 Hz, 1H), 2.30 (qd, *J* = 7.1, 2.7 Hz, 1H), 2.26 (d, *J* = 11.8 Hz, 1H), 2.23 (d, *J* = 14.3 Hz, 1H), 2.09 (ddt, *J* = 9.1, 6.7, 3.2 Hz, 2H), 2.08 – 2.03 (m, 0H), 2.00 (d, *J* = 14.4 Hz, 1H), 1.70 (t, *J* = 6.5 Hz, 1H), 1.55 – 1.48 (m, 2H), 1.44 (t, *J* = 7.3 Hz, 2H), 1.40 (td, *J* = 8.0, 4.9 Hz, 2H), 1.42 – 1.32 (m, 2H), 1.19 (d, *J* = 7.2 Hz, 3H), 1.06 (d, *J* = 6.9 Hz, 3H), 1.03 (td, *J* = 8.0, 5.5 Hz, 1H), 0.96 (t, *J* = 7.1 Hz, 3H), 0.95 (d, *J* = 7.1 Hz, 3H), 0.90 (d, *J* = 6.8 Hz, 3H), 0.89 – 0.83 (m, 1H), 0.69 (td, *J* = 8.4, 4.6 Hz, 1H), -0.09 (q, *J* = 5.3 Hz, 1H). ^{13}C NMR (126 MHz, Chloroform-*d*) δ 174.6, 167.7, 164.7, 163.7, 147.4, 132.6, 125.7, 112.7, 104.1, 99.9, 78.0, 75.7, 72.7, 72.0, 55.6, 44.9, 39.6, 39.2, 38.5, 37.8, 36.9, 36.0, 31.8, 31.2, 30.1, 19.4, 16.3, 16.1, 14.4, 14.3, 13.4, 11.3, 10.1, 8.8. HRMS (ESI/Q-TOF) m/z: $[M + H]^+$ Calcd for $C_{34}H_{54}NO_8$ 604.3844, found 604.3849. $[\alpha]^{20}_D$ = +3.46 (*c* = 0.09, DCM).

(2R,3S)-N-((5R,6R,7S,E)-7-((3S,8S,9R,Z)-9,14-dihydroxy-12-methoxy-8-methyl-1-oxo-3,4,7,8,9,10-hexahydro-1H-benzo[c][1]oxacyclododecin-3-yl)-6-hydroxy-5-methyloct-2-en-1-yl)-3-hydroxy-2-methylhexanamide (**16**): ^{1}H NMR (800 MHz, Chloroform-*d*) δ 11.49 (s, 1H), 6.37 (d, *J* = 2.7 Hz, 1H), 6.32 (d, *J* = 2.7 Hz, 1H), 5.85 (t, *J* = 5.8 Hz, 1H), 5.59 (dddt, *J* = 15.1, 7.9, 7.3, 1.5 Hz, 1H), 5.52 (ddd, *J* = 12.8, 10.7, 1.8 Hz, 1H), 5.49 – 5.39 (m, 2H), 5.27 (ddd, *J* = 11.7, 4.9, 1.9 Hz, 1H), 3.92 – 3.85 (m, 1H), 3.85 – 3.81 (m, 1H), 3.81 (s, 3H), 3.79 – 3.75 (m, 1H), 3.75 – 3.69 (m, 1H), 3.65 (dd, *J* = 11.0, 2.3 Hz, 1H), 3.45 (ddd, *J* = 8.6, 6.0, 2.5 Hz, 1H), 3.32 (d, *J* = 3.2 Hz, 1H), 2.89 – 2.83 (m, 1H), 2.33 (q, *J* = 14.3, 12.2, 12.0 Hz, 1H), 2.29 (qd, *J* = 7.1, 2.6 Hz, 2H), 2.27 – 2.23 (m, 1H), 2.19 (d, *J* = 13.8 Hz, 1H), 2.03 (ddt, *J* = 8.9, 6.6, 3.6 Hz, 2H), 1.97 (d, *J* = 14.5 Hz, 1H), 1.92 (ddd, *J* = 13.9, 8.0, 7.3 Hz, 1H), 1.68 – 1.62 (m, 1H), 1.61 (d, *J* = 6.0 Hz, 1H), 1.48 (ddd, *J* = 8.0, 5.2, 1.9 Hz, 2H), 1.37 (d, *J* = 2.8 Hz, 1H), 1.35 – 1.29 (m, 2H), 1.16 (d, *J* = 7.2 Hz, 3H), 1.03 (d, *J* = 6.9 Hz, 3H), 0.93 (t, *J* = 7.1 Hz, 3H), 0.92 (d, *J* = 7.1 Hz, 3H), 0.77 (d, *J* = 6.8 Hz, 3H). ^{13}C NMR (201 MHz, Chloroform-*d*) δ 176.3, 171.5, 165.7, 163.6, 143.6, 132.4, 131.7, 127.6, 125.5, 112.3, 104.9, 99.7, 77.8, 75.9, 73.1, 71.7, 55.4, 44.7, 41.1, 39.1, 38.2, 36.8, 36.7, 35.9, 35.7, 31.6, 29.9, 19.2, 16.1, 14.3, 14.0, 11.1, 8.5. HRMS (ESI/Q-TOF) m/z: $[M + H]^+$ Calcd for $C_{33}H_{52}NO_8$ 590.3687, found 590.3682. $[\alpha]^{20}_D$ = +4.62 (*c* = 0.22, DCM).

Statement of contributions

X.D. synthesized and purified cruentaren A and its analogues, characterized purified analogues via ^{1}H, ^{13}C, COSY, HSQC, HMBC, NOESY NMRs to identify the regioselective and stereoselective functionalization. H.G. purified ATP synthase, performed activity assays with the purified enzyme, performed the high-resolution cryo-EM structural studies, analyzed the resulting structures, and prepared supplementary figures. L.A. and C.S. performed the antiproliferative assays and the

Western Blot analysis. T. D. and B.A.P. provided cruentaren A and early-stage intermediates. All authors contributed to the data analysis. X.D. and H.G. wrote the manuscript. J.L.R. coordinated the structural studies and advised on cryoEM. M.C., J.L.R., B.S.J.B supervised the project.

Acknowledgments

This work was supported by the National Institutes of Health [grant number CA216919] and the Canadian Institutes of Health Research [grant number PJT162186]. This project was supported, in part, with support from the Indiana Clinical and Translational Sciences Institute (CTSI) funded, in part by Grant Number UL1TR002529 from the National Institutes of Health, National Center for Advancing Translational Sciences, Clinical and Translational Sciences Award. X.D. was supported by an Indiana CTSI Postdoctoral Challenge. H.G. was supported by an Ontario Graduate Scholarship for International Students. J.L.R. was supported by the Canada Research Chairs program. NMR data was collected at the Magnetic Resonance Research Center at the University of Notre Dame. CyroEM data was collected at the Toronto High-Resolution High-Throughput cryoEM facility, supported by the Canada Foundation for Innovation and Ontario Research Fund. The content is solely the responsibility of the authors and does not necessarily represent the official views of the National Institutes of Health.

Keywords

ATP synthase, Cruentaren A, natural product, cryoEM structure, late-stage modification

Supporting information

Supporting figures and table, materials and methods, experimental procedures, and characterization of chemical products including LCMS traces and NMR (^{1}H, ^{13}C, and 2D) spectra. CryoEM maps of yeast ATP synthase with 100 μM and 25 μM cruentaren A are deposited in the Electron Microscopy Data Bank under accession numbers EMD-28818 and EMD-28819, respectively. The atomic model is deposited in the Protein Data Bank under accession code 8F2K.

References

[1] a) L. Jundt, H. Steinmetz, P. Luger, M. Weber, B. Kunze, H. Reichenbach, G. Höfle, *Eur. J. Org. Chem.* **2006**, *2006*, 5036; b) B. Kunze, F. Sasse, H. Wieczorek, M. Huss, *FEBS Lett.* **2007**, *581*, 3523; c) B. Kunze, H. Steinmetz, G. Höfle, M. Huss, H. Wieczorek, H. Reichenbach, *J. Antibiot.* **2006**, *59*, 664.

[2] J. A. Hall, B. R. Kusuma, G. E. Brandt, B. S. Blagg, *ACS Chem. Biol.* **2014**, *9*, 976.

[3] P. M. M. Shelton, T. M. Kapoor, *Nat. Chem. Biol.* **2021**.

[4] a) J. Song, N. Pfanner, T. Becker, *Proc. Natl. Acad. Sci. U.S.A.* **2018**, *115*, 2850; b) J. He, H. C. Ford, J. Carroll, C. Douglas, E. Gonzales, S. Ding, I. M. Fearnley, J. E. Walker, *Proc. Natl. Acad. Sci. U.S.A.* **2018**, *115*, 2988.

[5] a) M. Bergeaud, L. Mathieu, A. Guillaume, U. Moll, B. Mignotte, N. Le Floch, J.-L. Vayssière, V. Rincheval, *Cell Cycle* **2013**, *12*, 2781; b) S. Yan, F. Du, L. Wu, Z. Zhang, C. Zhong, Q. Yu, Y. Wang, L.-F. Lue, D. G. Walker, J. T. Douglas, S. S. Yan, *Diabetes* **2016**, *65*, 3482; c) M. H. R. Ludtmann, P. R. Angelova, M. H. Horrocks, M. L. Choi, M. Rodrigues, A. Y. Baev, A. V. Berezhnov, Z. Yao, D. Little, B. Banushi, A. S. Al-

Menhali, R. T. Ranasinghe, D. R. Whiten, R. Yapom, K. S. Dolt, M. J. Devine, P. Gissen, T. Kunath, M. Jaganjac, E. V. Pavlov, D. Klenerman, A. Y. Abramov, S. Gandhi, *Nat. Commun.* **2018**, *9*, 2293; d) A. E. Papathanassiu, N. J. MacDonald, A. Bencsura, H. A. Vu, *Biochem. Biophys. Res. Commun.* **2006**, *345*, 419.
[6] a) S. K. Wandinger, K. Richter, J. Buchner, *J. Biol. Chem.* **2008**, *283*, 18473; b) C. Prodromou, *Curr. Top. Med. Chem.* **2009**, *9*, 1352; c) A. Kamal, L. Thao, J. Sensintaffar, L. Zhang, M. F. Boehm, L. C. Fritz, F. J. Burrows, *Nature* **2003**, *425*, 407.
[7] X. Dou, B. A. Patel, T. D'Amico, C. Subramanian, E. Cousineau, Y. Yi, M. Cohen, B. S. J. Blagg, *J. Org. Chem.* **2022**, *87*, 9940.
[8] J. P. Abrahams, A. G. W. Leslie, R. Lutter, J. E. Walker, *Nature* **1994**, *370*, 621.
[9] a) M. Bindl, L. Jean, J. Herrmann, R. Muller, A. Furstner, *Chem. Eur. J.* **2009**, *15*, 12310; b) V. V. Vintonyak, M. Cala, F. Lay, B. Kunze, F. Sasse, M. E. Maier, *Chem. Eur. J.* **2008**, *14*, 3709.
[10] D. B. Dess, J. C. Martin, *J. Org. Chem.* **1983**, *48*, 4155.
[11] L. A. Carpino, B. J. Cohen, K. E. Stephens, S. Y. Sadat-Aalaee, J. H. Tien, D. C. Langridge, *J. Org. Chem.* **1986**, *51*, 3732.
[12] L. A. Carpino, G. Y. Han, *J. Org. Chem.* **1972**, *37*, 3404.
[13] K. Oyama, T. Kondo, *Org. Lett.* **2003**, *5*, 209.
[14] T. J. Donohoe, K. Blades, P. R. Moore, M. J. Waring, J. J. Winter, M. Helliwell, N. J. Newcombe, G. Stemp, *J. Org. Chem.* **2002**, *67*, 7946.
[15] F. Song, S. Fidanze, A. B. Benowitz, Y. Kishi, *Tetrahedron* **2007**, *63*, 5739.
[16] V. VanRheenen, R. C. Kelly, D. Y. Cha, *Tetrahedron Lett.* **1976**, *17*, 1973.
[17] S. E. Denmark, J. P. Edwards, *J. Org. Chem.* **1991**, *56*, 6974.
[18] J. Yu, M. J. Gaunt, J. B. Spencer, *J. Org. Chem.* **2002**, *67*, 4627.
[19] a) B. Yucel, M. Sonmez, *Hematology* **2018**, *23*, 330; b) C. T. Hensley, B. Faubert, Q. Yuan, N. Lev-Cohain, E. Jin, J. Kim, L. Jiang, B. Ko, R. Skelton, L. Loudat, M. Wodzak, C. Klimko, E. McMillan, Y. Butt, M. Ni, D. Oliver, J. Torrealba, C. R. Malloy, K. Kernstine, R. E. Lenkinski, R. J. DeBerardinis, *Cell* **2016**, *164*, 681; c) B. Faubert, K. Y. Li, L. Cai, C. T. Hensley, J. Kim, L. G. Zacharias, C. Yang, Q. N. Do, S. Doucette, D. Burguete, H. Li, G. Huet, Q. Yuan, T. Wigal, Y. Butt, M. Ni, J. Torrealba, D. Oliver, R. E. Lenkinski, C. R. Malloy, J. W. Wachsmann, J. D. Young, K. Kernstine, R. J. DeBerardinis, *Cell* **2017**, *171*, 358.
[20] C. Erlichman, *Expert Opin. Investig. Drugs* **2009**, *18*, 861.
[21] J. Zou, Y. Guo, T. Guettouche, D. F. Smith, R. Voellmy, *Cell* **1998**, *94*, 471.
[22] Y. Xu, D. Xue, A. Bankhead, 3rd, N. Neamati, *J. Med. Chem.* **2020**, *63*, 14276.
[23] a) A. G. Atanasov, S. B. Zotchev, V. M. Dirsch, C. T. Supuran, *Nat. Rev. Drug. Discov.* **2021**, *20*, 200; b) B. Hong, T. Luo, X. Lei, *ACS Central Science* **2020**, *6*, 622.

Entry for the Table of Contents

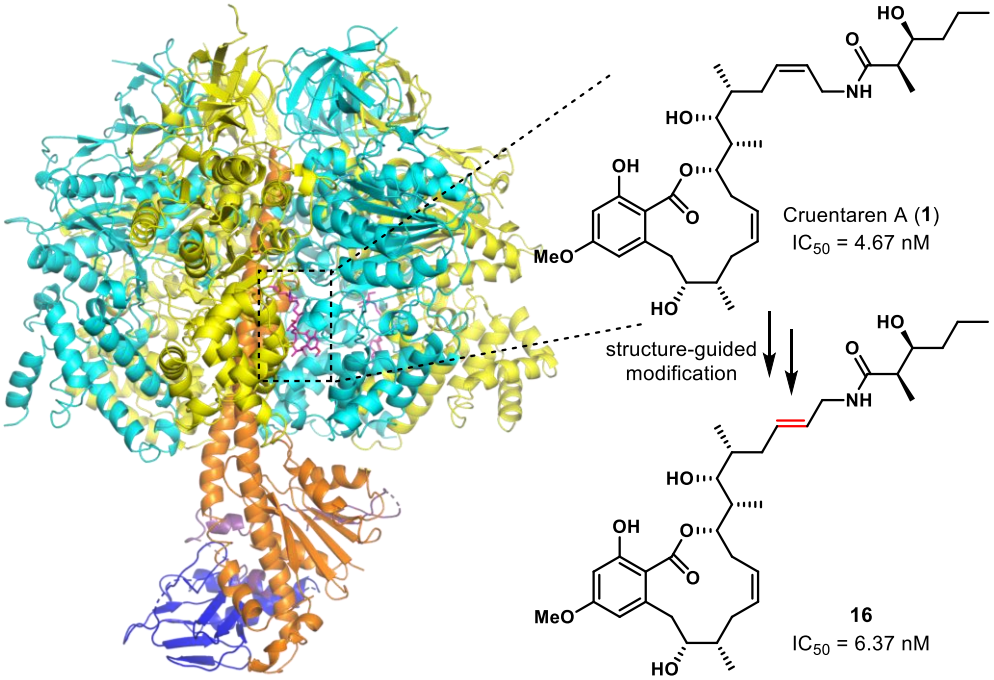

The cryogenic electron microscopy (cryoEM) structure of cruentaren A bound to ATP synthase is reported, which facilitated the design of new inhibitors via semisynthetic modification. Cruentaren A derivatives were developed, and a *trans*-alkene isomer was found to exhibit similar activity as cruentaren A against three cancer cell lines as well as other analogues that still retained potent inhibitory activity.